



Article

Novel PVDF-PVP Hollow Fiber Membrane Augmented with TiO₂ Nanoparticles: Preparation, Characterization and Application for Copper Removal from Leachate

Mohammed Umar Abba^{1,2}, Hasfalina Che Man^{1,3,*}, Raba'ah Syahidah Azis^{4,5}, Aida Isma Idris⁶, Muhammad Hazwan Hamzah^{1,3}, Khairul Faezah Yunos⁷ and Kamil Kayode Katibi^{1,8}

- ¹ Department of Biological and Agricultural Engineering, Faculty of Engineering, Universiti Putra Malaysia, Serdang 43400, Selangor, Malaysia; gs51611@student.upm.edu.my (M.U.A.); hazwanhamzah@upm.edu.my (M.H.H.); kamil.katibi@kwasu.edu.ng (K.K.K.)
 - ² Department of Agricultural and Bioenvironmental Engineering, Federal Polytechnic Mubi, Mubi 650221, Nigeria
 - ³ Smart Farming Technology Research Centre, Level 6, Blok Menara, Faculty of Engineering, Universiti Putra Malaysia, Serdang 43400, Selangor, Malaysia
 - ⁴ Department of Physics, Faculty of Science, Universiti Putra Malaysia, Serdang 43400, Selangor, Malaysia; rabaah@upm.edu.my
 - ⁵ Materials Synthesis and Characterization Laboratory (MSCL), Institute of Advanced Technology (ITMA), Universiti Putra Malaysia, Serdang 43400, Selangor, Malaysia
 - ⁶ Department of Chemical Engineering, Faculty of Engineering, Segi Universiti Malaysia, Petaling Jaya 47810, Selangor, Malaysia; aidaisma@segi.edu.my
 - ⁷ Department of Food and Process Engineering, Faculty of Engineering, Universiti Putra Malaysia, UPM, Serdang 43400, Selangor, Malaysia; kfaezah@upm.edu.my
 - ⁸ Department of Agricultural and Biological Engineering, Faculty of Engineering & Technology, Kwara State University, Malete, Ilorin 23431, Nigeria
- * Correspondence: hasfalina@upm.edu.my; Tel.: +60-3-97694340



Citation: Abba, M.U.; Man, H.C.; Azis, R.S.; Isma Idris, A.; Hazwan Hamzah, M.; Yunos, K.F.; Katibi, K.K. Novel PVDF-PVP Hollow Fiber Membrane Augmented with TiO₂ Nanoparticles: Preparation, Characterization and Application for Copper Removal from Leachate. *Nanomaterials* **2021**, *11*, 399. <https://doi.org/10.3390/nano11020399>

Academic Editor: Vincenzo Vaiano
Received: 8 January 2021
Accepted: 1 February 2021
Published: 4 February 2021

Publisher's Note: MDPI stays neutral with regard to jurisdictional claims in published maps and institutional affiliations.



Copyright: © 2021 by the authors. Licensee MDPI, Basel, Switzerland. This article is an open access article distributed under the terms and conditions of the Creative Commons Attribution (CC BY) license (<https://creativecommons.org/licenses/by/4.0/>).

Abstract: High proportion of copper has become a global challenge owing to its negative impact on the environment and public health complications. The present study focuses on the fabrication of a polyvinylidene fluoride (PVDF)-polyvinyl pyrrolidone (PVP) fiber membrane incorporated with varying loading (0, 0.5, 1.0, 1.5, and 2.0 wt%) of titanium dioxide (TiO₂) nanoparticles via phase inversion technique to achieve hydrophilicity along with high selectivity for copper removal. The developed fibers were characterized based on scanning electron microscopy (SEM), energy dispersive X-ray spectroscopy (EDX), permeability, porosity, zeta potential, and contact angle. The improved membrane (with 1.0 wt% TiO₂) concentration recorded the maximum flux (223 L/m²·h) and copper rejection (98.18%). Similarly, 1.0 wt% concentration of TiO₂ nanoparticles made the membrane matrix more hydrophilic with the least contact angle of 50.01°. The maximum copper adsorption capacity of 69.68 mg/g was attained at 1.0 wt% TiO₂ concentration. The experimental data of adsorption capacity were best fitted to the Freundlich isotherm model with R² value of 0.99573. The hybrid membrane developed in this study has considerably eliminated copper from leachate and the concentration of copper in the permeate was substantially reduced to 0.044 mg/L, which is below standard discharge threshold.

Keywords: hydrophilicity; porosity; copper adsorption; nanoparticles; agglomeration

1. Introduction

Leachate is a dark aqueous liquid generated from water passing through several layers of waste after undergoing a series of decomposition processes [1–3]. Heavy metals have been identified as one of the major constituents of leachate, which are harmful at high concentration with the propensity to accumulate in living organisms [4,5]. Notably, copper is an important trace element among the heavy metals that is essential for the

growth of plants, animals, and human being [6]. However, the accumulation of copper above the WHO permissible standard (1.3 mg/L) could trigger environmental and public health hazards such as kidney disorders and severe irritation of the gastrointestinal and nervous system in humans [7]. Excessive amounts of copper have been detected in agricultural soils, animal manures, and swine wastewater [8,9], with the possibility to impede the development of numerous aquatic fauna and flora and present critical difficulties to conventional treatment systems [8,10]. Additionally, high proportion of copper has been reported to possess the ability to ravage the natural environment [11–13]. Therefore, the treatment of landfill leachate is essential prior to discharge into natural water ways to mitigate environmental impacts.

Several techniques have been employed for the removal of copper from wastewater [14–17]. These techniques include adsorption [18,19], chemical precipitation [20], photocatalysis [21] coagulation-flocculation [22], and electrochemical treatment [23]. Most of these methods are energy consuming, require high operational and maintenance costs, and generate poisonous secondary sludge and liquid waste [24]. Several studies have focused on the adsorptive removal of Cu(II) via membranes [25,26]. The outstanding properties of membrane adsorption, including low energy requirement, small footprint, facile technique, and excellent filtration performance, have made it a suitable technique for the removal of copper from leachate [27–29]. However, deposition of foulants on the membrane surface is limiting the application of this technology [30]. Polymers have been the most exploited organic materials in membrane formulation, followed by the inorganic ones (e.g., metals, ceramics, and glass) [31]. Polymeric membranes are likely the most used membranes for water treatment with great design flexibility. Moreover, inorganic membranes, such as ceramic membranes, have high mechanical, thermal, and chemical stability [32]. As a present trend in the field of development of new membrane materials, the merging of both materials to fabricate nanocomposite membranes is also a promising tool for the efficient removal of heavy metals [33]. On this note, adsorptive membranes were fabricated by the use of polymers to enhance adsorption capability of membranes for heavy metals in particular copper removal from water and wastewater [34–36].

The metal oxide nanoparticles have been frequently used as an additive to increase the membrane performance [37]. Typically, numerous nanoparticles such as ZnO [38,39], TiO₂ [40,41], Ag₂O₃ [42,43], Al₂O₃ [44], graphene oxide [45,46], MgO [47], and CuO [48] are frequently employed for the manipulation of a polymeric membranes to augment its hydrophilicity properties. For instance, Song et al. [49] achieved a higher removal of nickel and copper by membrane separation using hydrophilic nanoparticles ion exchange barrier. Bandehali et al. [50] utilizes functionalized glycidyl nanoparticles to remove copper from water and achieved 86% rejection. Hosseini et al. [51] reported higher copper removal from water when activated carbon nanoparticles were used to modify membrane matrix. Kontoudakis et al. [52] removed copper from white wine by membrane filtration and recorded a significant reduction. Amongst the various nanoparticles, TiO₂ demonstrated a noticeable influence on the performance of the membranes for the removal of metal ions as reported from several studies [41,53–56]. The introduction of 1.0 wt% TiO₂ into membrane matrix structure improves the hydrophilicity and makes the surface more negatively charged. On this note, there is going to be electrostatic attraction between the negatively charged membrane surface and the positively charged heavy metals ions, thereby enhancing the adsorption efficacy. The reported impacts were attributed to the great affinity of TiO₂ toward heavy metals. Despite the potential of the membrane separation technology, the great affinity of TiO₂ towards heavy metals, and its capacity to increase membrane hydrophilic properties, information on the utilization of TiO₂ nanoparticles as a potent additive to modify PVDF-PVP membrane for the removal of copper from leachate continues to be very scanty. It is recommended that future research should focus on functionalizing the membrane matrix structure in order to address the problem of agglomeration so as to enhance flux and separation efficacy. In reflection of such interest, the present study fabricates a composite membrane blended with various concentrations

of TiO₂ nanoparticles via phase inversion method. The fabricated fibers were analyzed by means of SEM, EDX, FTIR, zeta potential, porosity, and contact angle. The flux and the copper rejection efficiency from feedwater (leachate) were also examined

2. Materials and Method

2.1. Experimental Materials

The materials used in the present study include *N, N*-dimethylacetamide (Dimethylacetamide (DMAc, Wako Pure Chemical Industries Ltd., Osaka, Japan), which was utilized devoid of additional purification to dissolve the polymer, and PVDF polymer pellets bought from Arkema (Kynar[®] 760 Inc., Philadelphia, PA, USA). As a co-polymer, PVP was employed to promote the creation of pores and was bought from Sigma-Aldrich (Milwaukee, WI 53209, USA) (MW = 10,000 Da). Sigma-Aldrich (Milwaukee, WI 53209, USA) supplied TiO₂ (Degussa P25, medium-sized particle size ~21 nm; heat shock pH 7, ≥98% analytic class) was used. The landfill leachate was sourced from a wastewater treatment facility situated in Negeri Sembilan, Selengor, Malaysia, into an airtight container.

2.1.1. Dope Preparation

The procedure employed in the membrane dope preparation has been explained in a previous study [41]. Table 1 present the proportions of solvents, polymers, additives, and nanoparticles used in the dope formulation.

Table 1. Dope chemical constituents.

| Membrane Constituents | Solvent (DMAc) (wt%) | Polymer (PVDF) (wt%) | Additive PVP (wt%) | TiO ₂ (wt%) |
|-----------------------|----------------------|----------------------|--------------------|------------------------|
| pure | 78.0 | 19.0 | 3.0 | 0.0 |
| (0.5) | 77.5 | 19.0 | 3.0 | 0.5 |
| (1.0) | 77.0 | 19.0 | 3.0 | 1.0 |
| (1.5) | 76.5 | 19.0 | 3.0 | 1.5 |
| (2.0) | 76.0 | 19.0 | 3.0 | 2.0 |

2.1.2. Nano-Composite PVDF-PVP-TiO₂-Fiber Membrane Spinning

The dope was conveyed into the annular spinneret utilizing the dry-jet wet spinning process [57]. The annular spinneret extrusion needle possessed an internal and external diameter of 0.55 and 1.15 mm. As the inside and outside coagulant, deionized and fresh water was used. The ultimate speed monitor, assembling drum velocity, extrusion rate, air distance, ambient temperature, outer coagulant temperature, and room humidity variables were all kept consistent at 7 rpm, 10 rpm, 5 mL/min, 10 cm, 25 °C, 29.5 ± 1 °C, and 72.7%. In a continuous flow water bath, the spun fibers were then soaked for 24 h to expel all the remaining solvents. Post-treatment was subsequently conducted to cushion constriction by dipping fibers for 12 h into an ethanol solution and then moved for another 5 h into a 10% aqueous glycerol. The fabricated membranes were air-dried at 60 °C for 24 h to ensure complete dehydration.

2.2. Analysis of Fabricated Membrane

2.2.1. Evaluation of Membrane Morphology

At a voltage of 20 Kv, the scanning electron microscopy (SEM) (Model: TM 3000, Hitachi, Tokyo, Japan) was used to capture the digital microstructure of the surface and the cross-sectional area of the whirled membranes. The cross-sectional imaging samples were initially frozen in liquid nitrogen. This is to promote acute fracturing and to guarantee a clearer framework. The shattered samples were covered with a slim gold coat and, subsequently, with a carbon tap, placed on the sample holder. The microstructures were subsequently tested with a SEM (S-3400, Hitachi, Tokyo, Japan) at an increased voltage of 20 kV.

2.2.2. Study of Energy Dispersive X-ray Spectroscopy (EDX)

Thermo Scientific was used for EDX assessment of membrane samples with varying TiO₂ loads; 1 g of fiber samples at various TiO₂ doses were used for EDX assessment employing SEM (TM 3000, Hitachi, Tokyo, Japan) to analyze the dimensions, dispersion, and elemental constituents of the fibers.

2.2.3. Analysis of Porosity

In determining the porosity of the membrane, the gravimetric approach was employed [40]. Approximately 40 cm of membrane samples were prepared, consisting of five (5) segments each. The open edges of the fibers were closed utilizing epoxy resin and then dipped at ambient temperature (25 ± 1 °C) in distilled water for 5 h. The soaked fibers were gently removed and then, using dry tissue paper, the tracks of water drops on the surface were mopped. The wet membrane (*M_w*) was used to measure the soaked-mopped fibers. The dipped membranes were then dried-out at 60 °C for 24 h and weighed as dry membrane (*M_d*). weight. The porosity (ϵ) of individual fibers was subsequently calculated utilizing Equation (1) [58,59].

$$\epsilon(\%) = \frac{1}{\rho_w} \left(\frac{M_w - M_d}{V} \right) \times 100 \quad (1)$$

where ϵ is the membrane porosity (%), ρ_w is the density of water, *M_w* is the weight of wet membrane, *M_d* is the weight of dry membrane, and *V* is the volume of the membrane specimen.

2.2.4. Analysis of Hydrophilicity

The hydrophilicity of the spun fibers was evaluated utilizing a goniometer (OCA 15EC, Data Physics, Succasunna, NJ, USA) relying on the water falling surface contact angle. Initially, a double-sided carbon tape was used, and a dried membrane sample was fastened tightly to the glass plate. Using the goniometer microneedle, approximately 1 µL of distilled water (contact liquid) was released on the membrane surface. The angle of the water droplets was automatically recorded by the instrument. The contact angle was calculated in replicates of 10 for each of the samples and the average mean value was taken into consideration. This method is intended to reduce the degree of data skew.

2.3. Membrane Efficiency Assessment

2.3.1. Flux Efficiency

To test filtration or permeability effectiveness, a dead-end filtration system kitted with a membrane module cell was utilized. A peristaltic pump (PLP 6000 produced by Dulabo Laborgeräte, Wertheim, Germany) supplied the membrane with the suction pressure. There are 20 membrane pieces with a uniform length of 35 cm in each of the modules. To ensure steady permeability, the membrane was firstly compressed for 30 min at a pressure of 0.4 MPa, while successive leachate filtration was carried out at a reduced pressure of 0.3 MPa. For a total filtration time of 200 min, the volume of the filtrate accumulated was evaluated at an interval of 50 min. Equation (2) was used to measure the flux of the whirled membranes that separate the pure water (*J_w*) and leachate (*J_L*).

$$R = \left(1 - \frac{C_p}{C_f} \right) \times 100 \quad (2)$$

where *R* is the copper removal (%) and *C_p* and *C_f* are the copper concentration in the filtrate (mg/L) and feed (mg/L).

2.3.2. Antifouling and Reutilization Evaluation

The resulting membranes were exposed to 3 filtration cycles with an operational period of 9 h overall. Each filtration cycle was completed under 200 min and was then applied again for an additional filtration cycle after a quick backwash using just 30 min of running tap water. Throughout the experiments, the flux (J_L) was calculated utilizing the corresponding volume of the filtrate obtained at an interval of 50 min. Based on the relative flux recovery (% RFR) and flux recovery ratio (% FRR), as stated in Equations (3) and (4), the antifouling efficiency of the membranes was evaluated [60–63].

$$\%RFR = \left[1 - \frac{J_L}{J_w} \right] \times 100 \quad (3)$$

$$\%FRR = \left(\frac{J_{w2}}{J_w} \right) \times 100 \quad (4)$$

where J_w is the water flux, J_L is the leachate flux, and J_{w2} is the re-evaluated pure water flux after cleaning (all in $L/m^2 \cdot h$).

2.4. Analysis of Zeta Potential

The zeta potential of fabricated membranes was assessed utilizing an electrokinetic analysis device from Anton Paar SurPASS (Berlin, Germany) using a flexible gap cell. The measurements were conducted utilizing an electrolyte solution refined at 0.1 M KCl with nitrogen. To change the pH level, 0.1 M NaOH and 0.05 M HCl were employed during the measurements.

2.5. Analytical Technique

Before and after treatment, the bicinchoninate method was used to evaluate the copper concentration present in the leachate. A 10 mL of leachate was filled into a sample cell. Cu Ver 1 copper reagent powder pillow was augmented to the sample cell. Within 30 min after the timer sounds the fabricated sample was inserted into the cell holding device of the ultraviolet–vis spectrophotometer (DR/4000u HACH, Loveland, CO, USA) at a wavelength of 560 nm to assess the concentration of copper in the leachate sample. Distilled water used in the experiments was sourced from the Milli-Q water refining device (18 MQ cm).

3. Results and Discussion

3.1. Impact of TiO_2 on Membrane Physical Properties

3.1.1. EDX Elemental Evaluation

Figure 1 exhibits the matrix structure and elemental constituents of the fabricated fibers. The neat membrane (Figure 1a), as shown in the elemental composition, has only oxygen and carbon on its structure, while membranes accreted with a TiO_2 dose of 0.5 wt% (Figure 1b) showed C, O, and Ti elemental composition. It was observed that with a rise in TiO_2 dosage in the dope, the Ti fraction in the elemental composition increased. Nevertheless, the O compositions decreased at greater TiO_2 dosage (2.0 wt%) as depicted in Figure 1e. As shown in Figure 1b,c, a free agglomeration is presented at 0.5 and 1.0 wt% TiO_2 concentration. Fibers with 1.5 and 2.0 wt% TiO_2 dosages (Figure 1d,e), on the other hand, exhibit heterogeneous dispersion and particle fragments, leading to agglomeration and viscosity upsurge in the dope [64].

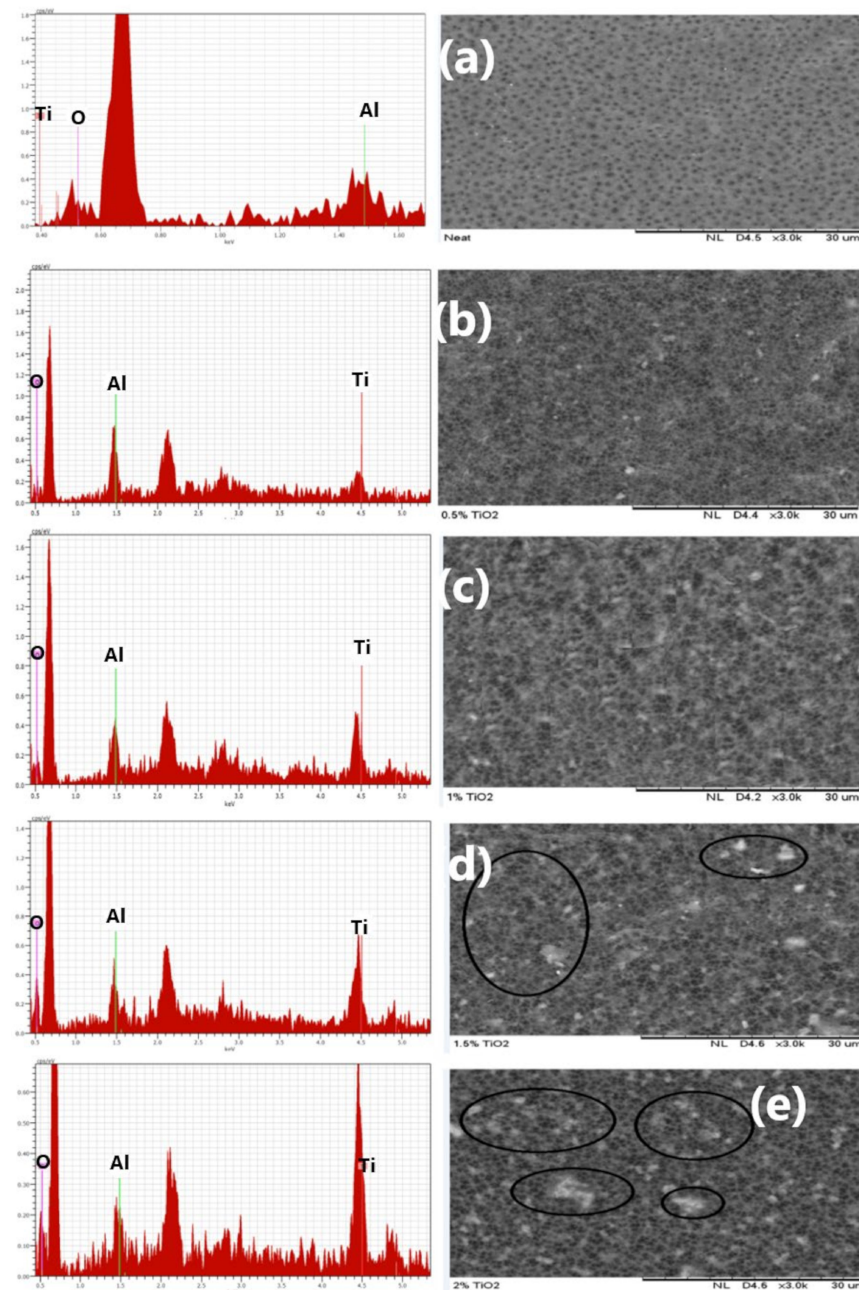


Figure 1. Matrix structure and elemental constituents of (a) neat TiO_2 , (b) 0.5 wt% TiO_2 , (c) 1.0 wt% TiO_2 , (d) 1.5 wt% TiO_2 , and (e) 2.0 wt% TiO_2 .

3.1.2. Morphological Structures

The scanning electron microscopy of the cross-section of different membranes fabricated with various TiO_2 doses is demonstrated in Figure 2. The incorporation of TiO_2 nanofillers into a membrane dope produces larger pores on the membrane matrix [65]. The finger-like pores of the improved membranes become bigger with increasing TiO_2 loading (0.5–2.0 wt%) as shown in Figure 2b,e [47]. This is attributed to the nucleation effects together with crosslinks produced amidst the TiO_2 and the polymeric materials [47]. However, from 0.5 to 1.0 wt%, uniform distribution of TiO_2 on the membrane matrix was observed as depicted in Figure 2a,c. Conversely, these nanoparticles appeared to agglomerate at a higher TiO_2 dosages (1.5 and 2 wt%) as shown in Figure 2d,e, and produced larger nanofillers, resulting in pore stoppage and decrease in water flux [66].

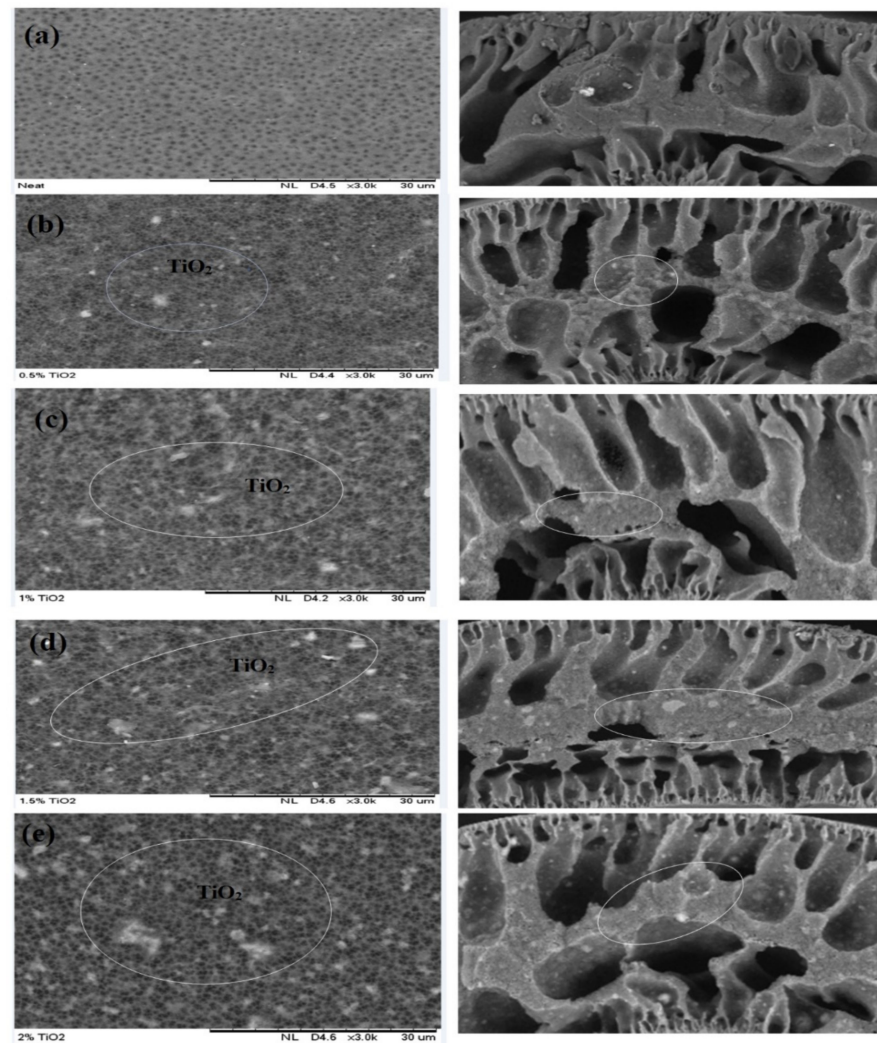


Figure 2. Scanning electron microscopy (SEM) images (cross and outer surface) of membranes fabricated with varying concentrations of TiO_2 : (a) neat TiO_2 , (b) 0.5 wt% TiO_2 , (c) 1.0 wt% TiO_2 , (d) 1.5 wt% TiO_2 , and (e) 2.0 wt% TiO_2 .

3.1.3. Evaluation of Hydrophilicity

Membrane surface hydrophilicity can be evaluated by determining the contact angle [67]. Figure 3 shows the contact angle of a neat and improved fibers. A strong distinction of both hydrophilicity and flux was rendered by the incorporation of TiO_2 nanofillers into the polymer dope solution [67]. At 1.0 wt% TiO_2 concentration, the modified membrane demonstrated the most hydrophilic with least contact angle of 50.01° , while the un-modified membrane recorded 66.7° . Further rise in TiO_2 dosage (1.5 and 2.0 wt%) results in the accumulation of nanoparticles inside the membrane matrix. This can be due to a heterogeneous dispersion of nanoparticles, a reduction in the surface potential, and a clogging of membrane pores [68,69]. The findings of the present and previous investigations revealed that the existence of TiO_2 nanoparticles in the matrix structure of the improved fibers enhances its hydrophilicity [41]. In addition, scholars have also revealed that most polymer membranes with strong hydrophilic characteristics are more likely to survive fouling [65,70].

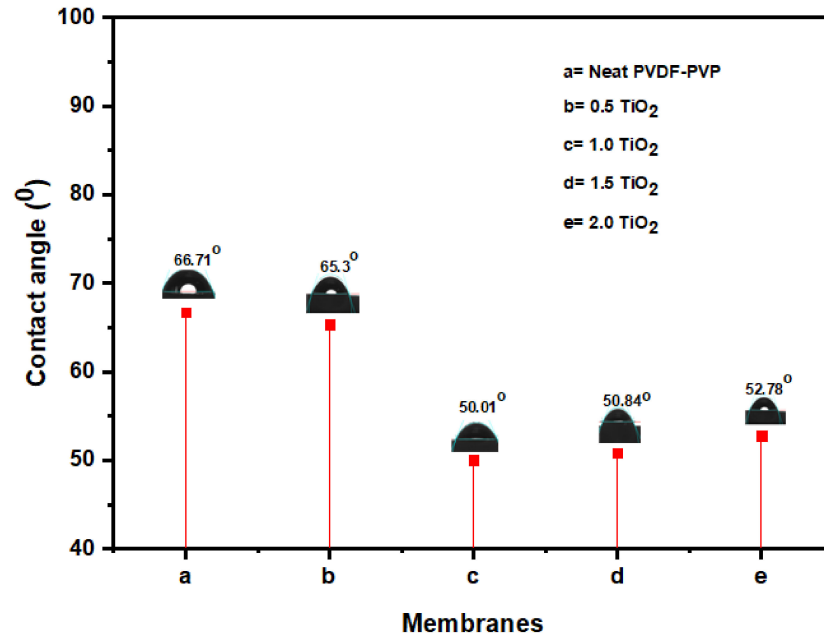


Figure 3. Membrane contact angle at various TiO₂ loading: (a) neat TiO₂, (b) 0.5 wt% TiO₂, (c) 1.0 wt% TiO₂, (d) 1.5 wt% TiO₂, and (e) 2.0 wt% TiO₂.

3.1.4. Zeta Potential

The surface charge of the neat and modified membranes was measured by a zeta potential analyzer. The surface zeta potential of the resultant membrane at various ranges of 2–10 pH is shown in Figure 4. Alongside increasing TiO₂ loading, the membrane matrix was more negatively charged. The TiO₂ exposed to the membrane surface has been hydrolyzed in the presence of water to form a functional hydroxide group, as depicted in Figure 4 TiO₂ protonation has led to deprotonation of the membrane surface [71]. Visibly, 1.0 wt% TiO₂ membrane had maximum negative zeta potential charge at pH 10 with −37 Mv. The hydrophilicity and zeta potential are critical variables in membrane analysis. The surface zeta potential of a membrane offers information about the membrane matrix surface charges which relies on the feed stream quality.

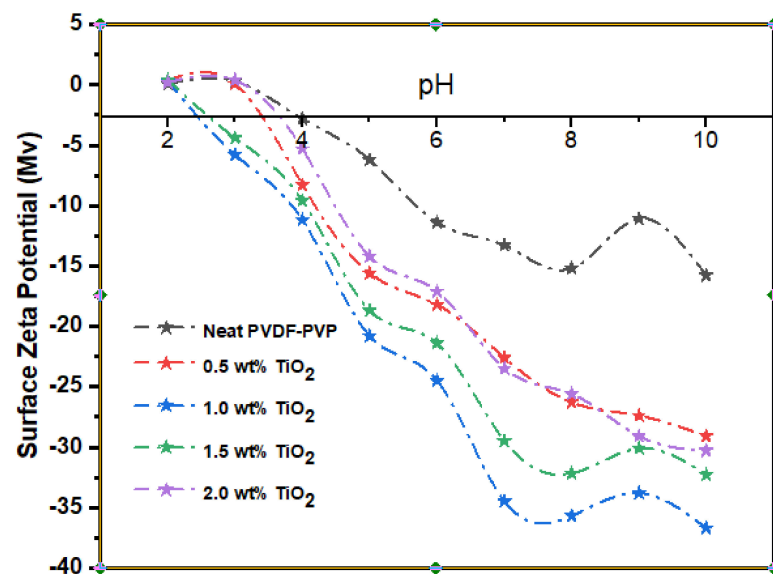


Figure 4. Membrane surface zeta potential at varying TiO₂ loading (0, 0.5 wt%, 1.0 wt%, 1.5 wt%, and 2.0 wt%).

3.1.5. Membrane Porosity

The result of membrane porosity has been described in our previous studies [41]. Based on this result, the porosity of the membrane is significantly influenced by TiO₂ loading rate in the dope solution. Additionally, the modified fibers with 1.0 wt% TiO₂ dosage exhibit superior porosity. Though, additional TiO₂ dosage (1.5–2.0 wt%) led to a decrease in porosity owing to rise in dope viscosity with lower pore volume [72,73]. The membrane with 2.0 wt% TiO₂ dosage had the least porosity among modified membranes. This may be attributed to the conglomeration and higher viscosity impact on the dope [74].

3.1.6. Permeability Flux

The effect of TiO₂ loading (0–2.0 wt%) on the membrane flux has been described in our previous studies [41]. It was noted that the flux for water and leachate filtration decreased to 207 and 156 L/m²·h at a higher load of TiO₂ nanoparticles (1.5 wt%). This is attributed to the nanoparticles' agglomerating effect on the membrane matrix [47], and heterogeneous dispersion of nanoparticles and obstruction of micropores on the surface of the membrane [68,69]. Moreover, the presence of agglomerated particles in the matrix structure could distort the additive's surface area interface (TiO₂) and initiate more roughness on the exterior surface of the [66]. Similarly, the membrane flux could be undermined due to the clogging of pores that impede water passage [66]. Generally, relative to pure water flux, the amount of flux in leachate was considerably lower due to the influence of more contaminants, particles, and colloidal objects in the leachate [38].

3.1.7. Copper Removal

The percentage of copper removal using neat and modified membranes under steady scouring aeration of 5 L/min is presented in Figure 5. The neat membrane had 96.36% copper removal in the first 20 min of filtration. At the initial filtration time, the removal performance fluctuated between 80–300 min. Thereafter, the percentage of copper removal remained stable at 340–400 min of filtration with 95.45% copper removal efficiency.

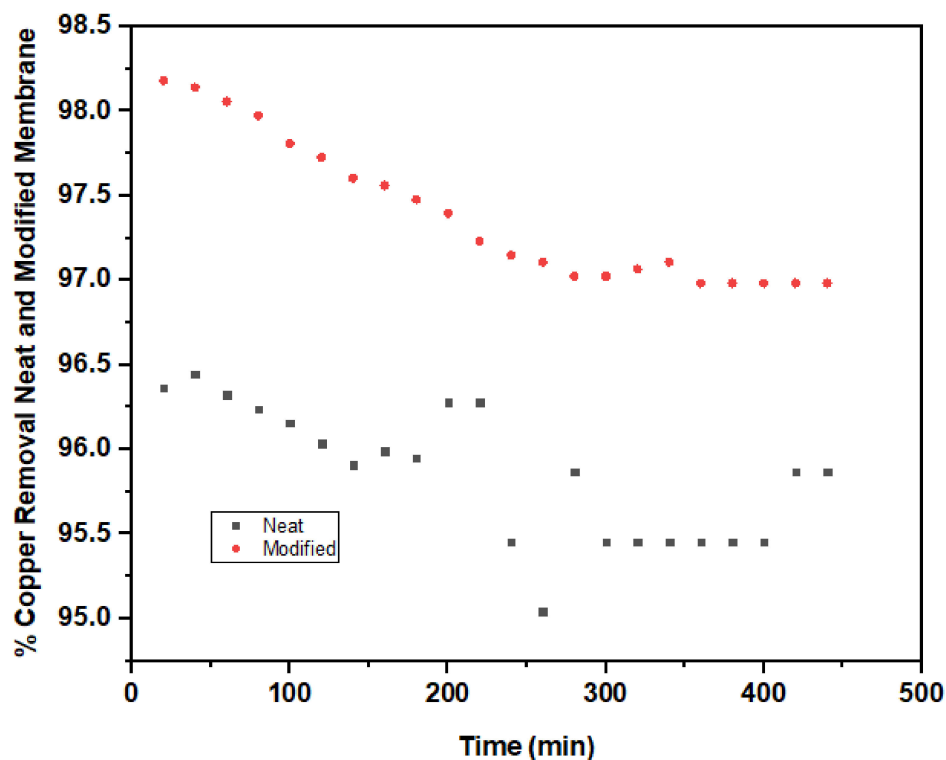


Figure 5. Copper removal by neat (PVDF-PVP) and modified (1.0 wt% TiO₂) membrane.

A significant improvement was noticed in the percentage of copper removal with 98.18% with a corresponding final concentration of 0.044 mg/L, which is far below 1.3 mg/L of WHO standard discharge limit for copper. Additionally, a steady removal performance was maintained at 360–440 min filtration duration with 96.98% removal rate. The percentage of copper removal recorded in the present study is in good agreement with the result obtained from [75] when a combined membrane filtration and electro dialysis treatment was used to remove copper from wafer polishing wastewater. Ghaemi et al. [74] introduced PPy@Al₂O₃ nanoparticles into polyethersulfone (PES) flat sheet membrane and significantly elevated copper removal during the membrane filtration.

3.1.8. Copper Removal Mechanism

The introduction of nanofillers onto the membrane matrix tailored the surface slightly more negatively [76,77]. The electrostatic attraction between the positively charged copper ions and the negatively charged membrane surface enhances copper adsorption. The positively charged copper ions are attracted to the negatively charged fiber matrix as depicted in Figure 6. The higher dispersion of nanoparticles on the membrane matrix led to an increase in the available sorption sites on the membrane surface [78]. The membranes could operate as an adsorptive barrier owing to the chemical structure of nanofillers, the augmentation of available active sites, and higher surface area determine the cation removal performance. The heavy metal ions in the feed solution can be captured by the adsorbent through the physical or chemical adsorption [79]. The treated permeate is collected and then subjected to analysis.

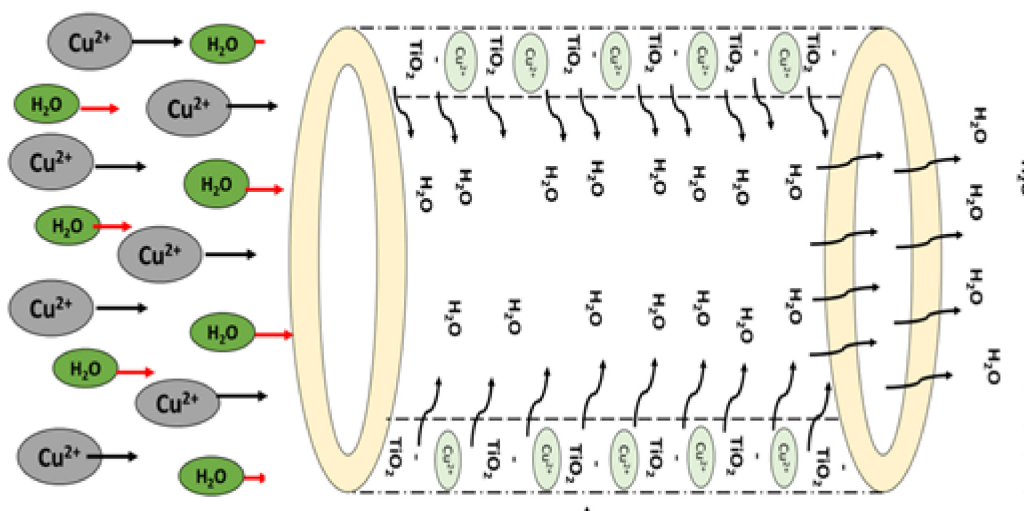


Figure 6. Copper removal mechanism on membrane matrix structure.

3.1.9. Adsorption of Copper by Modified Membrane

Adsorption is strongly linked to membrane pore radius, which permits most heavy metals with molecular weight less than the molecular cut off to access and diffuse into the membrane internal adsorption sites [80]. The occurrence of this mechanism is therefore mainly based on the amount of available adsorption sites at the surface of the membrane, together with the hydrophobicity of the compound. As earlier elucidated, the improved fiber with 1.0 wt% dosage is the most hydrophilic among the improved membranes. Hence, the adsorption capacity of copper into the modified membrane (1.0 wt% TiO₂) was studied as demonstrated in Figure 7c. The first 20 min filtration period recorded the maximum adsorption capacity (Q_{max}) of 69.68 mg/g. The result obtained is attributed to the availability of active pore sites, which enhances the adsorption process. The higher adsorption capacity recorded in this study was consistent with the findings from [26]. The adsorption capacity had a slight decline and remained stable after 340 min filtration period. The slight

reduction in adsorption capacity was due to membrane fouling. The experimental data of adsorption capacity were best fitted to the Freundlich isotherm model with an R^2 value of 0.99573 as depicted in Figure 7b.

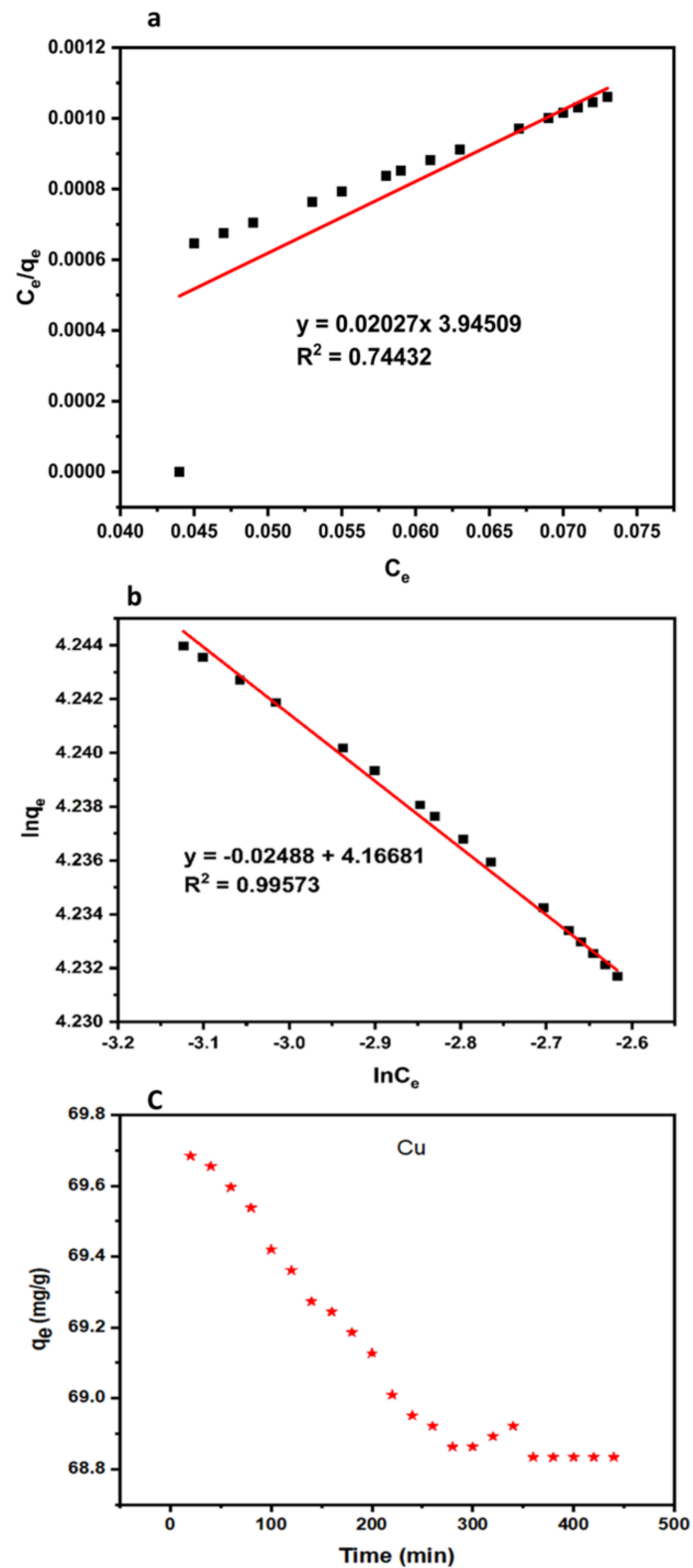


Figure 7. Langmuir (a), Freundlich isotherm, (b) and copper adsorption capacity (c) into hollow fiber membrane at pH 10, time 440 min, and initial copper concentration 2.42 mg/L.

3.1.10. Evaluation of Membrane Fouling

The effects of flux in three filtration cycles with regard to time are shown in Figure 8. Noticeably, there was a decrease in flux for all the fabricated membranes, including membranes modified with varied TiO_2 dosages (0–2.0 wt%) over time as a result of the accumulation of foulants on the surface of the membranes. The unmodified fibers had a flux of $89 \text{ L/m}^2\cdot\text{h}$, while the transformed membrane with 1.0 wt% TiO_2 recorded a flux of $157 \text{ L/m}^2\cdot\text{h}$ after 200 min of operation. A decline in permeability flux of 77 and $138 \text{ L/m}^2\cdot\text{h}$ was noticed for the neat and modified membranes, respectively. Hydrophobic membranes are much more vulnerable to fouling due to the effective adhesive attraction between the collaborating interfaces [69]. Foulant deposition can be resolved by incorporating hydrophilic nanofillers into the membrane matrix. The membranes were substantially washed for 30 min after each filtration cycle under flowing tap water.

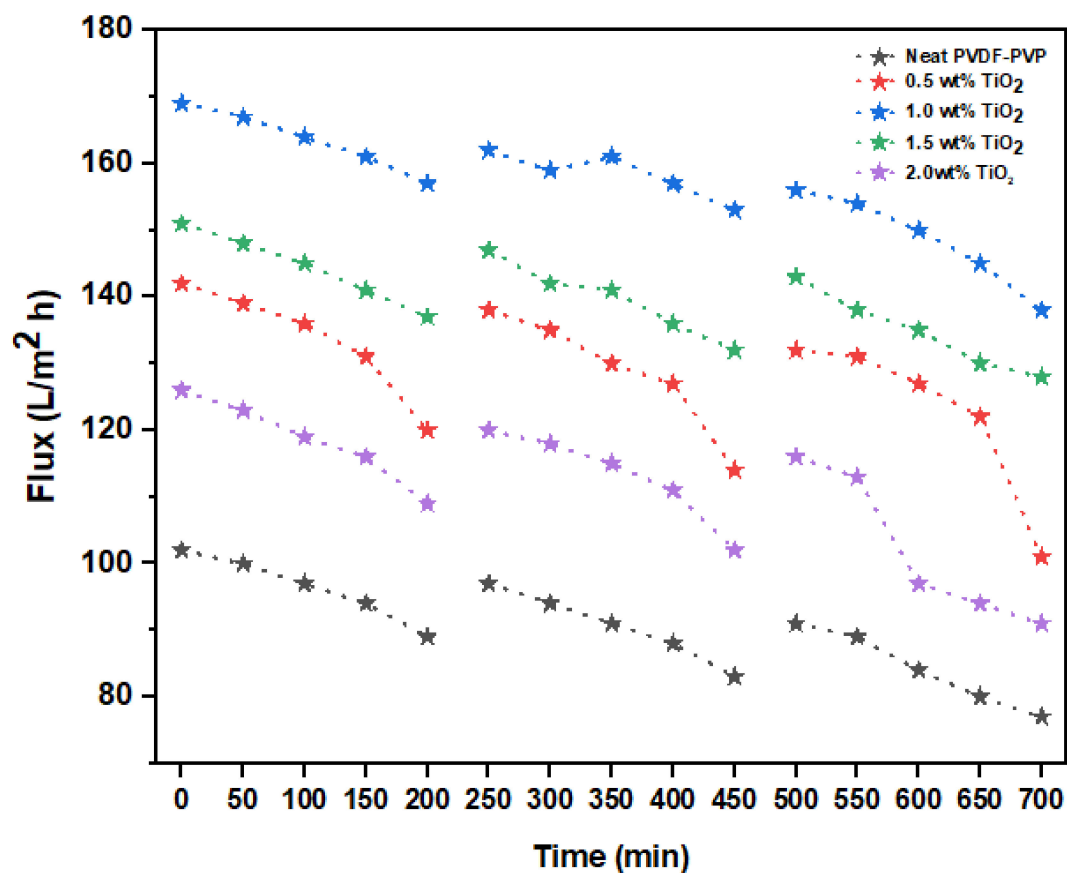


Figure 8. Antifouling characteristics of neat and modified membranes (0.5, 1.0, 1.5, and 2.0 wt% TiO_2).

3.1.11. Performance Evaluation with Literature

Information on comparison of the current study with previous studies on adsorptive removal of heavy metals by membrane is provided in this section. The result of the present study revealed that dispersion of 1.0 wt% TiO_2 concentration into PVDF-PVP dope improves the membrane performance in terms of contact angle (50.01°), flux ($223 \text{ L/m}^2\cdot\text{h}$), and copper adsorption capacity (69.68 mg/g). Mundal and Kumar [81] fabricated polysulfone-based hybrid ultrafiltration membranes for the adsorptive removal of Pb^{2+} ions from polluted aqueous solutions; 279.63 mg/g was obtained as the highest adsorptive capacity for the feed concentration of 200 mg/L , and the permeate flux of 1.65 mL min^{-1} . However, despite higher adsorption capacity, the permeate flux is relatively low. Additionally, Abdullah et al. [82] utilized polysulfone/hydrous ferric oxide ultrafiltration mixed matrix membrane for the adsorptive removal of lead (II) from aqueous solution. The result of

the study showed that the highest adsorption capacity of Pb(II) was 13.2 mg/g. Similarly, Adam et al. [83] employed novel natural zeolite based hollow fiber ceramic membrane for the adsorptive removal of chromium (VI) in aqueous solution. The performance of the resultant membrane in adsorption-filtration was 44% of Cr (VI) removal at the Cr (VI) concentration of 40 mg/L and pH 4. However, the copper removal efficiency was very low.

A comparative study on the adsorptive removal of copper by membrane in the present study and other literatures is presented in Table 2. The high adsorption capacity recorded in the present study could be attributed to the small pore size and high surface area of the TiO₂ nanoparticles. The present study fills a knowledge gap, considering the fact that information on the utilization of TiO₂ nanoparticles as a potent additive to modify PVDF-PVP membrane for the removal of copper from leachate continues to be very scanty.

Table 2. Comparison of adsorptive removal of heavy metals by membrane.

| Membrane | Removal Mechanism | Pollutant | q _e (mg/g) | Re (%) | Remark | Reference |
|-----------------------------|-------------------|------------------|-----------------------|--------|--|---------------|
| Hollow fiber | Adsorption | Cu ²⁺ | 92.38 | NA | The Langmuir isotherm model best fitted the adsorption isotherms | [84] |
| Polysulfone Ultrafiltration | Adsorption | Cu ²⁺ | 279.63 | ND | Impressive adsorption capacity | [81] |
| Ultrafiltration membrane | Adsorption | Cu ²⁺ | 2.82 | 97 | The membrane has removed Cu (II) from water at low pressure | [85] |
| Adsorptive membranes | Adsorption | Cu ²⁺ | 20.1 | | The results suggested that the membrane can remove copper | [86] |
| PES modified membrane | Adsorption | Cu ²⁺ | NA | 92 | Higher copper removal achieved | [87] |
| PVDF/ZnO hybrid membranes | Adsorption | Cu (II) ion | 11 | ND | Better adsorption and desorption properties for copper ions | [88] |
| PVDF-PVP-TiO ₂ | Adsorption | Cu ²⁺ | 69.68 | 98.18 | WHO standard achieved | Present study |

NA = Not available.

4. Conclusions

This study demonstrated the preparation and characterization of PVDF-PVP hollow fiber membrane impregnated with TiO₂ nanoparticles and their potential ability to remove copper from leachate. The nanoparticles improve the membrane negative surface potential and enhance their permeability due to increased membrane porosity. The fabricated membrane blended with TiO₂ nanoparticles at varied concentrations (0–2.0 wt%). Notably, fibers improved with 1.0 wt% dosage exhibited higher flux of 223 L/m²h and 172 L/m²h for pure water and leachate. The high porosity of 85.50% recorded at 1.0 wt% loading of TiO₂ nanoparticles into the membrane matrix resulted in improvement in surface hydrophilicity relative to the pristine membrane. Furthermore, the modified membrane (1.0 wt%) is more hydrophilic with the least contact angle of 50.01° and superior copper rejection (98.18%) together with higher copper adsorption capacity of 69.69 mg/g. The experimental data of adsorption capacity were best fitted to the Freundlich isotherm model with an R² value of 0.99573. The present study concluded that the nanoparticle additives improve the membrane porosity, flux, copper adsorption and rejection, hydrophilicity, and antifouling properties. Hence, the developed hybrid PVDF-PVP membrane modified with 1.0 wt% TiO₂ can be successfully used for the treatment of industrial effluent-containing copper ions.

Author Contributions: Conceptualization, M.U.A. and H.C.M. methodology, M.U.A., H.C.M., R.S.A., and K.K.K.; software, M.U.A.; validation, M.U.A., A.I.I., M.H.H., R.S.A., K.F.Y. and H.C.M.; formal analysis, M.U.A., H.C.M., and R.S.A.; investigation, M.U.A.; data curation, M.U.A.; writing—original draft preparation, M.U.A.; writing—review and editing, M.U.A., H.C.M., R.S.A., M.H.H., and K.F.Y.; visualization, M.U.A., H.C.M., and M.H.H.; supervision, H.C.M., R.S.A., M.H.H., and A.I.I.; project administration, H.C.M., R.S.A., and M.H.H.; funding acquisition, R.S.A., H.C.M., and M.U.A. All authors have read and agreed to the published version of the manuscript.

Funding: The authors would like to gratefully acknowledge Universiti Putra Malaysia (UPM) for the financial support of this work via UPM/700-1/2/GPPI/2017/954160 and 9580600.

Institutional Review Board Statement: Not applicable.

Informed Consent Statement: Not applicable.

Data Availability Statement: Not applicable.

Acknowledgments: The authors would like to gratefully acknowledge Universiti Putra Malaysia (UPM) for supporting and financing this work in the preparation, execution, and write-up.

Conflicts of Interest: The authors declare no conflict of interest.

References

1. Robinson, A.H. Landfill leachate treatment. *Membr. Technol.* **2005**, *2005*, 6–12. [[CrossRef](#)]
2. Abbas, A.A.; Jingsong, G.; Ping, L.Z.; Ya, P.Y.; Al-Rekabi, W.S. Review on Landfill Leachate Treatments. *J. Appl. Sci. Res.* **2009**, *5*, 534–545.
3. Wiszniowski, J.; Robert, D.; Surmacz-Gorska, J.; Miksch, K.; Weber, J.V. Landfill leachate treatment methods: A review. *Environ. Chem. Lett.* **2006**, *4*, 51–61. [[CrossRef](#)]
4. Adani, F. Biostabilization of mechanically. *Waste Manag. Res.* **2000**, *18*, 471–477. [[CrossRef](#)]
5. Lee, A.H.; Nikraz, H.; Hung, Y.T. Influence of Waste Age on Landfill Leachate Quality. *Int. J. Environ. Sci. Dev.* **2010**, *1*, 347–350. [[CrossRef](#)]
6. Kumar, M.; Shevate, R.; Hilke, R.; Peinemann, K.V. Novel adsorptive ultrafiltration membranes derived from polyvinyltetrazole-co-polyacrylonitrile for Cu(II) ions removal. *Chem. Eng. J.* **2016**, *301*, 306–314. [[CrossRef](#)]
7. Taylor, A.A.; Tsuji, J.S.; Garry, M.R.; McArdle, M.E.; Goodfellow, W.L.; Adams, W.J.; Menzie, C.A. Critical Review of Exposure and Effects: Implications for Setting Regulatory Health Criteria for Ingested Copper. *Environ. Manag.* **2020**, *65*, 131–159. [[CrossRef](#)]
8. Du, H.; Harata, N.; Li, F. Responses of riverbed sediment bacteria to heavy metals: Integrated evaluation based on bacterial density, activity and community structure under well-controlled sequencing batch incubation conditions. *Water Res.* **2018**, *130*, 115–126. [[CrossRef](#)]
9. Ji, X.; Shen, Q.; Liu, F.; Ma, J.; Xu, G.; Wang, Y.; Wu, M. Antibiotic resistance gene abundances associated with antibiotics and heavy metals in animal manures and agricultural soils adjacent to feedlots in Shanghai; China. *J. Hazard. Mater.* **2012**, *235*, 178–185. [[CrossRef](#)]
10. Tandon, S.A.; Kumar, R.; Yadav, S.A. Pytoremediation of fluoroquinolone group of antibiotics from waste water. *Nat. Sci.* **2013**, *5*, 21–27. [[CrossRef](#)]
11. Wen, S.; Liu, H.; He, H.; Luo, L.; Li, X.; Zeng, G.; Zhou, Z.; Lou, W.; Yang, C. Treatment of anaerobically digested swine wastewater by *Rhodobacter blasticus* and *Rhodobacter capsulatus*. *Bioresour. Technol.* **2016**, *222*, 33–38. [[CrossRef](#)] [[PubMed](#)]
12. Wang, J.; Chen, C. Biosorbents for heavy metals removal and their future. *Biotechnol. Adv.* **2009**, *27*, 195–226. [[CrossRef](#)] [[PubMed](#)]
13. Yin, Y.; Gu, J.; Wang, X.; Song, W.; Zhang, K.; Sun, W.; Zhang, X.; Zhang, Y.; Li, H. Effects of copper addition on copper resistance, antibiotic resistance genes, and intl1 during swine manure composting. *Front. Microbiol.* **2017**, *8*, 1–10. [[CrossRef](#)]
14. Ren, Z.; Zhang, W.; Meng, H.; Liu, J.; Wang, S. Extraction separation of Cu(II) and Co(II) from sulfuric solutions by hollow fiber renewal liquid membrane. *J. Memb. Sci.* **2010**, *365*, 260–268. [[CrossRef](#)]
15. Ku, Y.; Chen, S.W.; Wang, W.Y. Effect of solution composition on the removal of copper ions by nanofiltration. *Sep. Purif. Technol.* **2005**, *43*, 135–142. [[CrossRef](#)]
16. Tizaoui, C.; Rachmawati, S.D.; Hilal, N. The removal of copper in water using manganese activated saturated and unsaturated sand filters. *Chem. Eng. J.* **2012**, *209*, 334–344. [[CrossRef](#)]
17. AbuDalo, M.A.; Nevostrueva, S.; Hernandez, M.T. Enhanced Copper (II) Removal from Acidic Water By Granular Activated Carbon Impregnated with Carboxybenzotriazole. *APCBEE Procedia* **2013**, *5*, 64–68. [[CrossRef](#)]
18. Ben-Ali, S.; Jaouali, I.; Souissi-Najar, S.; Ouederni, A. Characterization and adsorption capacity of raw pomegranate peel biosorbent for copper removal. *J. Clean. Prod.* **2017**, *142*, 3809–3821. [[CrossRef](#)]
19. Lee, C.G.; Lee, S.; Park, J.A.; Park, C.; Lee, S.J.; Kim, S.B.; An, B.; Yun, S.T.; Lee, S.H.; Choi, J.W. Removal of copper, nickel and chromium mixtures from metal plating wastewater by adsorption with modified carbon foam. *Chemosphere* **2017**, *166*, 203–211. [[CrossRef](#)]
20. Rojas, R. Copper, lead and cadmium removal by Ca Al layered double hydroxides. *Appl. Clay Sci.* **2014**, *87*, 254–259. [[CrossRef](#)]

21. Kanakaraju, D.; Ravichandar, S.; Lim, Y.C. Combined effects of adsorption and photocatalysis by hybrid TiO₂/ZnO-calcium alginate beads for the removal of copper. *J. Environ. Sci. China* **2017**, *55*, 214–223. [[CrossRef](#)]
22. Hargreaves, A.J.; Vale, P.; Whelan, J.; Alibardi, L.; Constantino, C.; Dotro, G.; Cartmell, E.; Campo, P. Coagulation–flocculation process with metal salts, synthetic polymers and biopolymers for the removal of trace metals (Cu, Pb, Ni, Zn) from municipal wastewater. *Clean Technol. Environ. Policy* **2018**, *20*, 393–402. [[CrossRef](#)]
23. Feng, Y.; Yang, L.; Liu, J.; Logan, B.E. Electrochemical technologies for wastewater treatment and resource reclamation. *Environ. Sci. Water Res. Technol.* **2016**, *2*, 800–831. [[CrossRef](#)]
24. Al-Saydeh, S.A.; El-Naas, M.H.; Zaidi, S.J. Copper removal from industrial wastewater: A comprehensive review. *J. Ind. Eng. Chem.* **2017**, *56*, 35–44. [[CrossRef](#)]
25. Shen, S.S.; Yang, J.J.; Liu, C.X.; Bai, R.B. Immobilization of copper ions on chitosan/cellulose acetate blend hollow fiber membrane for protein adsorption. *RSC Adv.* **2017**, *7*, 10424–10431. [[CrossRef](#)]
26. Mondal, M.; Dutta, M.; De, S. A novel ultrafiltration grade nickel iron oxide doped hollow fiber mixed matrix membrane: Spinning, characterization and application in heavy metal removal. *Sep. Purif. Technol.* **2017**, *188*, 155–166. [[CrossRef](#)]
27. Hamiche, A.M.; Stambouli, A.B.; Flazi, S. A review of the water-energy nexus. *Renew. Sustain. Energy Rev.* **2016**, *65*, 319–331. [[CrossRef](#)]
28. Goh, P.S.; Matsuura, T.; Ismail, A.F.; Ng, B.C. The Water–Energy Nexus: Solutions towards Energy-Efficient Desalination. *Energy Technol.* **2017**, *5*, 1136–1155. [[CrossRef](#)]
29. Zeng, G.; Ye, Z.; He, Y.; Yang, X.; Ma, J.; Shi, H.; Feng, Z. Application of dopamine-modified halloysite nanotubes/PVDF blend membranes for direct dyes removal from wastewater. *Chem. Eng. J.* **2017**, *323*, 572–583. [[CrossRef](#)]
30. Katibi, K.K.; Yunos, K.F.; Man, H.C.; Aris, A.Z.; Zuhair, M.; Syahidah, R. Recent Advances in the Rejection of Endocrine-Disrupting Compounds from Water Using Membrane and Membrane Bioreactor Technologies: A Review. *Polymers* **2021**, *13*, 392. [[CrossRef](#)]
31. Ulbricht, M. Advanced functional polymer membranes. *Polym. Guildf.* **2006**, *47*, 2217–2262. [[CrossRef](#)]
32. Galiano, F.; Drioli, E.; Figoli, A. Mixed matrix membranes (MMMs) for ethanol purification through pervaporation: Current state of the art. *Rev. Chem. Eng.* **2018**, *13*. [[CrossRef](#)]
33. Loreti, L.; Castro-Muñoz, R. Ongoing progress on novel nanocomposite membranes for the separation of heavy metals from contaminated water. *Chemosphere* **2021**, *270*. [[CrossRef](#)]
34. Salehi, E.; Daraei, P.; Arabi Shamsabadi, A. A review on chitosan-based adsorptive membranes. *Carbohydr. Polym.* **2016**, *152*, 419–432. [[CrossRef](#)] [[PubMed](#)]
35. Boricha, A.G.; Murthy, Z.V.P. Acrylonitrile butadiene styrene/chitosan blend membranes: Preparation, characterization and performance for the separation of heavy metals. *J. Memb. Sci.* **2009**, *339*, 239–249. [[CrossRef](#)]
36. Cheng, Z.; Liu, X.; Han, M.; Ma, W. Adsorption kinetic character of copper ions onto a modified chitosan transparent thin membrane from aqueous solution. *J. Hazard. Mater.* **2010**, *182*, 408–415. [[CrossRef](#)]
37. Ng, L.Y.; Mohammad, A.W.; Leo, C.P.; Hilal, N. Polymeric membranes incorporated with metal/metal oxide nanoparticles: A comprehensive review. *Desalination* **2013**, *308*, 15–33. [[CrossRef](#)]
38. Tan, Y.H.; Goh, P.S.; Ismail, A.F.; Ng, B.C.; Lai, G.S. Decolourization of aerobically treated palm oil mill effluent (AT-POME) using polyvinylidene fluoride (PVDF) ultrafiltration membrane incorporated with coupled zinc-iron oxide nanoparticles. *Chem. Eng. J.* **2017**, *308*, 359–369. [[CrossRef](#)]
39. Zinadini, S.; Rostami, S.; Vatanpour, V.; Jalilian, E. Preparation of antibiofouling polyethersulfone mixed matrix NF membrane using photocatalytic activity of ZnO/MWCNTs nanocomposite. *J. Memb. Sci.* **2017**, *529*, 133–141. [[CrossRef](#)]
40. Subramaniam, M.N.; Goh, P.S.; Lau, W.J.; Tan, Y.H.; Ng, B.C.; Ismail, A.F. Hydrophilic hollow fiber PVDF ultrafiltration membrane incorporated with titanate nanotubes for decolourization of aerobically-treated palm oil mill effluent. *Chem. Eng. J.* **2017**, *316*, 101–110. [[CrossRef](#)]
41. Man, H.C.; Abdulsalam, M.; Abba, M.U.; Syahidah, R. Utilization of Nano-TiO₂ as an influential additive for Complementing Separation Performance of a Hybrid PVDF-PVP Hollow Fiber: Boron removal from leachate. *Polymers* **2020**, *12*, 2511. [[CrossRef](#)] [[PubMed](#)]
42. Li, J.H.; Shao, X.S.; Zhou, Q.; Li, M.Z.; Zhang, Q.Q. The double effects of silver nanoparticles on the PVDF membrane: Surface hydrophilicity and antifouling performance. *Appl. Surf. Sci.* **2013**, *265*, 663–670. [[CrossRef](#)]
43. Mauter, M.S.; Okemgbo, K.C.; Osuji, C.O.; Elimelech, M.; Wang, Y.; Giannelis, E.P. Antifouling ultrafiltration membranes via post-fabrication grafting of biocidal nanomaterials. *ACS Appl. Mater. Interfaces* **2011**, *3*, 2861–2868. [[CrossRef](#)] [[PubMed](#)]
44. Jhaveri, J.H.; Murthy, Z.V.P. A comprehensive review on anti-fouling nanocomposite membranes for pressure driven membrane separation processes. *Desalination* **2016**, *379*, 137–154. [[CrossRef](#)]
45. Meng, F.; Zhang, S.; Oh, Y.; Zhou, Z.; Shin, H.S.; Chae, S.R. Fouling in membrane bioreactors: An updated review. *Water Res.* **2017**, *114*, 151–180. [[CrossRef](#)] [[PubMed](#)]
46. Chae, H.R.; Lee, J.; Lee, C.H.; Kim, I.C.; Park, P.K. Graphene oxide-embedded thin-film composite reverse osmosis membrane with high flux, anti-biofouling, and chlorine resistance. *J. Memb. Sci.* **2015**, *483*, 128–135. [[CrossRef](#)]
47. Abdulsalam, M.; Man, H.C.; Goh, P.S.; Yunos, K.F.; Abidin, Z.Z.; Aida Isma, M.I.; Ismail, A.F. Permeability and Antifouling Augmentation of a Hybrid PVDF-PEG Membrane Using Nano-Magnesium Oxide as a Powerful Mediator for POME Decolorization. *Polym. Guildf.* **2020**, *12*, 549. [[CrossRef](#)] [[PubMed](#)]

48. Nasrollahi, N.; Vatanpour, V.; Aber, S.; Mahmoodi, N.M. Preparation and characterization of a novel polyethersulfone (PES) ultrafiltration membrane modified with a CuO/ZnO nanocomposite to improve permeability and antifouling properties. *Sep. Purif. Technol.* **2018**, *192*, 369–382. [[CrossRef](#)]
49. Song, J.; Niu, X.; Li, X.M.; He, T. Selective separation of copper and nickel by membrane extraction using hydrophilic nanoporous ion-exchange barrier membranes. *Process Saf. Environ. Prot.* **2018**, *113*, 1–9. [[CrossRef](#)]
50. Bandehali, S.; Parvizian, F.; Moghadassi, A.R.; Hosseini, S.M. Copper and lead ions removal from water by new PEI based NF membrane modified by functionalized POSS nanoparticles. *J. Polym. Res.* **2019**, *26*, 211. [[CrossRef](#)]
51. Hosseini, S.M.; Amini, S.H.; Khodabakhshi, A.R.; Bagheripour, E.; Van Der Bruggen, B. Activated carbon nanoparticles entrapped mixed matrix polyethersulfone based nanofiltration membrane for sulfate and copper removal from water. *J. Taiwan Inst. Chem. Eng.* **2018**, *82*, 169–178. [[CrossRef](#)]
52. Kontoudakis, N.; Mierczynska-Vasilev, A.; Guo, A.; Smith, P.A.; Scollary, G.R.; Wilkes, E.N.; Clark, A.C. Removal of sulfide-bound copper from white wine by membrane filtration. *Aust. J. Grape Wine Res.* **2018**, 1–9. [[CrossRef](#)]
53. Contreras, A.R.; García, A.; González, E.; Casals, E.; Puentes, V.; Sánchez, A.; Font, X.; Recillas, S. Potential use of CeO₂, TiO₂ and Fe₃O₄ nanoparticles for the removal of cadmium from water. *Desalin. Water Treat.* **2012**, *41*, 296–300. [[CrossRef](#)]
54. Recillas, S.; García, A.; González, E.; Casals, E.; Puentes, V.; Sánchez, A.; Font, X. Use of CeO₂, TiO₂ and Fe₃O₄ nanoparticles for the removal of lead from water. Toxicity of nanoparticles and derived compounds. *Desalination* **2011**, *277*, 213–220. [[CrossRef](#)]
55. Faghih Nasiri, E.; Yousefi Kebria, D.; Qaderi, F. An Experimental Study on the Simultaneous Phenol and Chromium Removal from Water Using Titanium Dioxide Photocatalyst. *Civ. Eng. J.* **2018**, *4*, 585. [[CrossRef](#)]
56. Poursani, A.S.; Nilchi, A.; Hassani, A.; Shariat, S.M.; Nouri, J. The Synthesis of Nano TiO₂ and Its Use for Removal of Lead Ions from Aqueous Solution. *J. Water Resour. Prot.* **2016**, *8*, 438–448. [[CrossRef](#)]
57. Li, S.; Zhu, Q.; Sun, Y.; Wang, L.; Lu, J.; Nie, Q.; Ma, Y.; Jing, W. Fabrication of Ag nanosheet @ TiO₂ antibacterial membranes for inulin purification. *Ind. Eng. Chem. Res.* **2020**. [[CrossRef](#)]
58. Fan, L.; Shi, J.; Xi, Y. PVDF-Modified Nafion Membrane for Improved Performance of MFC. *Membranes* **2020**, *10*, 185. [[CrossRef](#)]
59. Wang, H.; Gong, R.; Qian, X. Preparation and characterization of TiO₂/g-C₃N₄/PVDF composite membrane with enhanced physical properties. *Membranes* **2018**, *8*, 14. [[CrossRef](#)]
60. Razmjou, A.; Mansouri, J.; Chen, V. The effects of mechanical and chemical modification of TiO₂ nanoparticles on the surface chemistry, structure and fouling performance of PES ultrafiltration membranes. *J. Memb. Sci.* **2011**, *378*, 73–84. [[CrossRef](#)]
61. Zhang, F.; Zhang, W.; Yu, Y.; Deng, B.; Li, J.; Jin, J. Sol-gel preparation of PAA-g-PVDF/TiO₂ nanocomposite hollow fiber membranes with extremely high water flux and improved antifouling property. *J. Memb. Sci.* **2013**, *432*, 25–32. [[CrossRef](#)]
62. Zeng, G.; He, Y.; Yu, Z.; Zhan, Y.; Ma, L.; Zhang, L. Preparation and characterization of a novel PVDF ultrafiltration membrane by blending with TiO₂-HNTs nanocomposites. *Appl. Surf. Sci.* **2016**, *371*, 624–632. [[CrossRef](#)]
63. Liu, Y.; Xiao, T.; Bao, C.; Zhang, J.; Yang, X. Performance and fouling study of asymmetric PVDF membrane applied in the concentration of organic fertilizer by direct contact membrane distillation (DCMD). *Membranes* **2018**, *8*, 9. [[CrossRef](#)] [[PubMed](#)]
64. Hikku, G.S.; Jeyasubramanian, K.; Vignesh Kumar, S. Nanoporous MgO as self-cleaning and anti-bacterial pigment for alkyd based coating. *J. Ind. Eng. Chem.* **2017**, *52*, 168–178. [[CrossRef](#)]
65. Liu, Q.; Huang, S.; Zhang, Y.; Zhao, S. Comparing the antifouling effects of activated carbon and TiO₂ in ultrafiltration membrane development. *J. Colloid Interface Sci.* **2018**, *515*, 109–118. [[CrossRef](#)]
66. Méricq, J.P.; Mendret, J.; Brosillon, S.; Faur, C. High performance PVDF-TiO₂ membranes for water treatment. *Chem. Eng. Sci.* **2015**, *123*, 283–291. [[CrossRef](#)]
67. Han, B.; Liang, S.; Wang, B.; Zheng, J.; Xie, X.; Xiao, K.; Wang, X.; Huang, X. Simultaneous determination of surface energy and roughness of dense membranes by a modified contact angle method. *Colloids Surf. A Physicochem. Eng. Asp.* **2019**, *562*, 370–376. [[CrossRef](#)]
68. Zhu, Z.; Jiang, J.; Wang, X.; Huo, X.; Xu, Y.; Li, Q.; Wang, L. Improving the hydrophilic and antifouling properties of polyvinylidene fluoride membrane by incorporation of novel nanohybrid GO@SiO₂ particles. *Chem. Eng. J.* **2017**, *314*, 266–276. [[CrossRef](#)]
69. Jayalakshmi, A.; Kim, I.; Kwon, Y. Suppression of gold nanoparticle agglomeration and its separation via nylon membranes. *Chin. J. Chem. Eng.* **2017**, *25*, 931–937. [[CrossRef](#)]
70. Bae, T.H.; Tak, T.M. Effect of TiO₂ nanoparticles on fouling mitigation of ultrafiltration membranes for activated sludge filtration. *J. Memb. Sci.* **2005**, *249*, 1–8. [[CrossRef](#)]
71. Pedersen, M.L.K.; Jensen, T.R.; Kucheryavskiy, S.V.; Simonsen, M.E. Investigation of surface energy, wettability and zeta potential of titanium dioxide/graphene oxide membranes. *J. Photochem. Photobiol. A Chem.* **2018**, *366*, 162–170. [[CrossRef](#)]
72. Taylor, P.; Ong, C.S.; Lau, W.J.; Goh, P.S.; Ng, B.C.; Matsuura, T.; Ong, C.S.; Lau, W.J.; Goh, P.S.; Ng, B.C.; et al. Effect of PVP Molecular Weights on the Properties of PVDF-TiO₂ Composite Membrane for Oily Wastewater Treatment Process. *Sep. Sci. Technol.* **2014**, *49*, 37–41. [[CrossRef](#)]
73. Simone, S.; Galiano, F.; Faccini, M.; Boerrigter, M.E.; Chaumette, C.; Drioli, E.; Figoli, A. Preparation and Characterization of Polymeric-Hybrid PES/TiO₂ Hollow Fiber Membranes for Potential Applications in Water Treatment. *Fibers* **2017**, *5*, 14. [[CrossRef](#)]
74. Liu, C.; Lee, J.; Small, C.; Ma, J.; Elimelech, M. Comparison of organic fouling resistance of thin-film composite membranes modified by hydrophilic silica nanoparticles and zwitterionic polymer brushes. *J. Memb. Sci.* **2017**, *544*, 135–142. [[CrossRef](#)]

75. Su, Y.N.; Lin, W.S.; Hou, C.H.; Den, W. Performance of integrated membrane filtration and electro dialysis processes for copper recovery from wafer polishing wastewater. *J. Water Process Eng.* **2014**, *4*, 149–158. [[CrossRef](#)]
76. Ghaemi, N.; Daraei, P. Enhancement in copper ion removal by PPy@Al₂O₃ polymeric nanocomposite membrane. *J. Ind. Eng. Chem.* **2016**, *40*, 26–33. [[CrossRef](#)]
77. Teow, Y.H.; Ooi, B.S.; Ahmad, A.L. Study on PVDF-TiO₂ mixed-matrix membrane behaviour towards humic acid adsorption. *J. Water Process Eng.* **2017**, *15*, 99–106. [[CrossRef](#)]
78. Ghaemi, N.; Madaeni, S.S.; Daraei, P.; Rajabi, H.; Zinadini, S.; Alizadeh, A.; Heydari, R.; Beygzadeh, M.; Ghouzivand, S. *Polyethersulfone Membrane Enhanced with Iron Oxide Nanoparticles for Copper Removal from Water: Application of New Functionalized Fe₃O₄ Nanoparticles*; Elsevier: Amsterdam, The Netherlands, 2015; Volume 263, ISBN 6814989468.
79. Khulbe, K.C.; Matsuura, T. *Removal of Heavy Metals and Pollutants by Membrane Adsorption Techniques*; Springer: Berlin/Heidelberg, Germany, 2018; Volume 8, ISBN 0123456789.
80. Roy, D.; Khosravanipour Mostafazadeh, A.; Drogui, P.; Tyagi, R.D. *Removal of Organic Micro-Pollutants by Membrane Filtration*; Elsevier: Amsterdam, The Netherlands, 2020; ISBN 9780128195949.
81. Mondal, S.; Majumder, S.K. Fabrication of the polysulfone-based composite ultra filtration membranes for the adsorptive removal of heavy metal ions from their contaminated aqueous solutions. *Chem. Eng. J.* **2020**, *401*, 126036. [[CrossRef](#)]
82. Abdullah, N.; Gohari, R.J.; Yusof, N.; Ismail, A.F.; Juhana, J.; Lau, W.J.; Matsuura, T. Polysulfone / hydrous ferric oxide ultrafiltration mixed matrix membrane: Preparation, characterization and its adsorptive removal of lead (II) from aqueous solution. *Chem. Eng. J.* **2016**, *289*, 28–37. [[CrossRef](#)]
83. Ridhwan, M.; Mohd, N.; Ha, M.; Othman, D.; Matsuura, T.; Ha, M.; Ha, M.; Ismail, A.F.; Rahman, M.A. The adsorptive removal of chromium (VI) in aqueous solution by novel natural zeolite based hollow fibre ceramic membrane. *J. Environ. Manag.* **2018**, *224*, 252–262. [[CrossRef](#)]
84. He, Z.; Huang, Q.; Mao, L.; Huang, H.; Liu, M.; Chen, J.; Deng, F.; Zhou, N.; Zhang, X.; Wei, Y. Direct surface modification of nanodiamonds with ionic copolymers for fast adsorptive removal of copper ions with high efficiency. *Colloids Interface Sci. Commun.* **2020**, *37*, 100278. [[CrossRef](#)]
85. Abd Hamid, S.; Shahadat, M.; Ballinger, B.; Farhan Azha, S.; Ismail, S.; Wazed Ali, S.; Ziauddin Ahammad, S. Role of clay-based membrane for removal of copper from aqueous solution. *J. Saudi Chem. Soc.* **2020**, *24*, 785–798. [[CrossRef](#)]
86. Salehi, E.; Madaeni, S.S.; Rajabi, L.; Vatanpour, V.; Derakhshan, A.A.; Zinadini, S.; Ghorabi, S.; Ahmadi Monfared, H. Novel chitosan/poly(vinyl) alcohol thin adsorptive membranes modified with amino functionalized multi-walled carbon nanotubes for Cu(II) removal from water: Preparation, characterization, adsorption kinetics and thermodynamics. *Sep. Purif. Technol.* **2012**, *89*, 309–319. [[CrossRef](#)]
87. Kashif, M.; Phearom, S.; Choi, Y. Chemosphere Synthesis of magnetite from raw mill scale and its application for arsenate adsorption from contaminated water. *Chemosphere* **2018**, *203*, 90–95. [[CrossRef](#)]
88. Zhang, X.; Wang, Y.; Liu, Y.; Xu, J.; Han, Y.; Xu, X. Preparation, performances of PVDF/ZnO hybrid membranes and their applications in the removal of copper ions. *Appl. Surf. Sci.* **2014**, *316*, 333–340. [[CrossRef](#)]